Available online at www.sciencedirect.com

SCIENCE DIRECT®

Journal of Photochemistry and Photobiology A: Chemistry 171 (2005) 69–76

Journal of Photochemistry and Photobiology A:Chemistry

www.elsevier.com/locate/jphotochem

The relationship between the electrochemical and photochemical reduction of some azo dyes derived from 2-aminobenzothiazole

R. Podsiadły[a], J. Sokołowska[a,*], A. Marcinek[b,*], J. Zielonka[b], A. Socha[c], M. Kaźmierska[d]

[a] *Department of Dyes, Technical University, Zeromskiego 116, 90-924 Lodz, Poland*
[b] *Institute of Applied Radiation Chemistry, Technical University, Zeromskiego 116, 90-924 Lodz, Poland*
[c] *Institute of General and Ecological Chemistry, Technical University, Zeromskiego 116, 90-924 Lodz, Poland*
[d] *Institute of Dyes and Organic Products, Chemikow 2/4, 95-100 Zgierz, Poland*

Received 16 June 2004; received in revised form 22 September 2004; accepted 24 September 2004
Available online 28 October 2004

Abstract

Electrochemical and photochemical experiments in ethanol show that the tendency to the reduction of some azo dyes derived from 2-aminobenzothiazole is parallel for both processes. This is attributed to the one-electron reduction of the dyes followed by a protonation of the resulting radical anions. The primary transient products of the reduction process, i.e. the radical anions, and their reactivity are characterized in solution at ambient temperature and under matrix conditions at 77 K by means of pulse radiolysis.

Keywords: 2-Aminobenzothiazole; Azo dyes; Electrochemical reduction; Photochemical reduction; Pulse radiolysis

1. Introduction

Heterocycles are mainly used in disperse dye chemistry as diazo or coupling components and numerous heterocyclic colorants are widely marketed. In addition new application appeared such as photodynamic therapy, laser industry or reprographic technology [1–4]. Although the heterocyclic azo dyes represent a large group of synthetic colorants their photochemistry has not been studied as well as other group of the dyes.

The photolytic behaviour of the dye depends on many factors such as its chemical structure and the external conditions [5–10]. It is well known from open literature that depending on the fibre photoreduction or photooxidation processes of the same dye are observed [11]. Reduction processes play an important role in the photofading of azo dyes and in case of nitro-substituted dyes, which show a strong decrease in the light stability, may involve both the azo and the nitro group. In this paper we investigate in details the effect of nitro substitution on the reduction process of the azo dyes derived from 2-aminobenzothiazole.

The key objective of this study is to present the relationship between photochemical, electrochemical and radiolytic reduction of dyes **1**–**3**, since the photolytic reactions are often associated with the tendency of the colorants to the chemical reduction/oxidation. The argument for this approach is the Becquerel effect [12] observed for the irradiated solutions of some selected dyes.

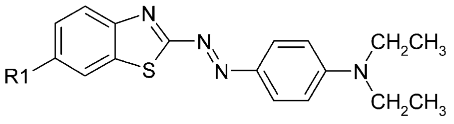

---

[*] Corresponding authors. Tel.: +48 42 631 31 68; fax: +48 42 636 50 08 (A. Marcinek)/+48 42 636 25 96 (J. Sokołowska).

E-mail addresses: jsokolow@p.lodz.pl (J. Sokołowska), marcinek@p.lodz.pl (A. Marcinek).

1010-6030/$ – see front matter © 2004 Elsevier B.V. All rights reserved.
doi:10.1016/j.jphotochem.2004.09.009

Dye	R1
1	H
2	OCH_3
3	NO_2

Table 2
Calculated electron affinities of the ground (EA) and triplet excited (EA_{trip}) states of the dyes **1**–**3**

Dye	EA [eV]	EA_{trip} [eV]
1	1.23	1.90
2	1.16	1.82
3	1.91	2.56

2. Experimental

2.1. The synthesis

The azo dyes **1**–**3** were prepared by diazotisation of the appropriate amine with nitrosyl sulphuric acid [13] followed by coupling reaction and purified by recrystallisation (toluene). The purity of the final compound was checked by TLC [Merck Silica gel 60, eluent: toluene–ethyl acetate 3:1 (v/v)]. The chemical structures of the dyes were confirmed by ^{1}H NMR. The ^{1}H NMR spectra were recorded on Bruker Avance DPX 250 spectrometer at 250.13 MHz in $CDCl_3$ solutions using TMS as internal standard.

2.1.1. Preparation of the dye **1**

2-Aminobenzothiazole (3.0 g, 0.02 mol) was dissolved in 17 ml of acetic acid at 30 °C, diluted with 12 ml H_2O followed by addition of 1.8 ml of conc. H_2SO_4. The reaction mixture was cooled to 0 °C and nitrosyl sulphuric acid [formed by dissolving 1.6 g (0.023 mol) of $NaNO_2$ in 10 ml of conc. H_2SO_4 at 70 °C] was added over 1 h. After stirring for 1.5 h the mixture was diluted with 60 g of ice, followed by addition of *N*,*N*-diethylaniline (3.2 ml, 0.02 mol) in 10 ml of acetic acid at a rate such that the reaction temperature did not exceed 2 °C. After stirring for 2 h the precipitated dye was filtered off, washed with water and dried. Three grams of the dye was obtained; yield: 48%.

2.1.2. Preparation of the dye **2**

6-Methoxy-2-aminobenzothiazole (3.8 g, 0.02 mol) was added at 0–5 °C to the nitrosyl sulphuric acid solution which was prepared by dissolving 1.5 g (0.02 mol) of $NaNO_2$ in 10 ml of conc. H_2SO_4 at 70 °C, followed by addition of acetic and propionic acids mixture [20 ml, 17:3 (v/v)] at 15 °C. Then the additional 20 ml of the same mixture was added and the diazotisation was carried out for 2.5 h. The resulting diazonium salt was added dropwise at 0–5 °C to the solution of *N*,*N*-diethylaniline (3.2 ml, 0.02 mol) in 40 ml of acetic and propionic acids mixture and the coupling was continued for 1 h. The reaction mixture was diluted with 60 g of ice, the precipitated dye was filtered off, washed with water and dried. 3.8 g of the dye was obtained; yield: 55%.

2.1.3. Preparation of the dye **3**

2-Amino-6-nitrobenzothiazole (3.9 g, 0.02 mol) was dissolved in 30 ml of 85% H_3PO_4. The reaction mixture was cooled to −5 °C and then $NaNO_2$ (1.4 g, 0.02 mol) was added over 1 h. Diazotisation was continued for 1 h. The resulting diazonium salt was added dropwise at 0–5 °C into the solution of *N*,*N*-diethylaniline (3.2 ml, 0.02 mol) in 1 ml of acetic acid. The coupling was continued for 2 h. Then the reaction mixture was diluted with 60 g of ice and the precipitated dye was filtered off, washed with water and dried. Three grams of the dye was obtained; yield: 46%.

The ^{1}H NMR data, mp, λ_{max}, log ε of dyes **1**–**3** are presented in Table 1.

2.2. Quantum chemical calculations

The geometries of all species were optimised by the B3LYP density functional method [14,15] as implemented in the Gaussian 98 suite of programs [16]. The above calculations were done for the ground and triplet states of the dyes, and neutral radicals with the standard 6-31G* basis set.

The calculations of electron affinities (EAs) were limited only to the vertical EA, i.e. the difference in relative energies of neutral parent dye and its radical anion obtained by single point calculations at B3LYP/6-31 + G* level for the same optimised geometry of neutral compound (Table 2).

2.3. Electrochemical reduction

The electrochemical experiments were carried out in EtOH and DMF solutions containing 0.1 mol/l of tetra-*n*-

Table 1
Melting points, visible spectral data[a] and ^{1}H NMR spectral data[b] of dyes **1**–**3**

	mp [°C]	λ_{max} [nm]	log ε	^{1}H NMR ($CDCl_3$), δ (ppm), J (Hz)
1	160	513	4.68	1.27 t (6H, $J = 7.5$), 3.50 q (4H, $J = 7.5$), 6.74 d (2H, $J = 10$), 7.37–7.49 m (2H), 7.83 d (1H, $J = 7.5$), 7.98 d (2H, $J = 10$), 8.06 d (1H, $J = 7.5$)
2	158	515	4.70	1.26 t (6H, $J = 7.5$), 3.49 q (4H, $J = 7.5$), 3.90 s (3H), 6.75 d (2H, $J = 10$), 7.06 dd (1H, J 2.5, $J = 10$), 7.28 d (1H, $J = 2.5$), 7.94–7.97 d (3H, $J = 10$)
3	177	549	4.44	1.30 t (6H, $J = 7.5$), 3.54 q (4H, $J = 7.5$), 6.77 d (2H, $J = 10$), 7.99 d (2H, $J = 10$), 8.08 d (1H, $J = 7.5$), 8.31 dd (1H, $J = 2.5$, $J = 10$), 8.73 d (1H, $J = 2.5$)

[a] In EtOH.

[b] Abbreviations: s, singlet; d, doublet; t, triplet; q, quartet; m, multiplet; b, broad.

butylammonium perchlorate as a supporting electrolyte. All solutions were degassed prior to experiments by bubbling with argon. During each experiment, a blanket of argon was maintained over the solution. The concentration of the dyes was 10^{-3} mol/l. The staircase voltammetry technique (SCV) [17] was used. The experiments were carried out with the use of the potentiostat AUTOLAB (Ecochemie, Holland). Working hanging mercury drop electrode, platinum auxiliary electrode and ferrocene reference electrode [18,19] were used. The current was measured at half width step and d*E* was 2.0 mV [17].

2.4. Photochemical experiments

Dye solutions (5×10^{-5} mol/l) in freshly distilled EtOH and DMF were faded in a Rayonet photolytic reactor RPR200 (Southern New England Ultraviolet Co) equipped with 14 300 nm lamps. Anaerobic conditions were achieved by bubbling with dry nitrogen into the solution for 30 min before irradiation. The extent of fading was determined according to the decrease in absorption at λ_{max} of the dye. The concentration of the remaining dye was determined spectrophotometrically. The spectra were recorded on Lambda 40 spectrophotometer (Perkin Elmer). The illumination intensity was determined using uranyl oxalate actinometry [20]. The Φ values were estimated from at least two determinations at 7% extent of the reaction.

2.5. Distribution coefficient measurements

To a 5 ml portion of the solvent (DMF, MeOH), 5 ml of immiscible *n*-hexane and a known quantity of dyes were added. The mixture was shaken and then thermostatted. After 12 h the concentration of the dye in equilibrium was determined in both phases by measuring their absorbances. The distribution coefficients γ were calculated directly from the ratio of the absorbances.

2.6. Pulse radiolysis of room-temperature liquids

Pulse radiolysis experiments were carried out with high energy (6 MeV) 17 ns electron pulses generated from ELU-6 linear electron accelerator. The dose absorbed per pulse was determined with N_2O saturated aqueous solution of KSCN (0.01 M), assuming $G((SCN)_2^{\bullet-}) = 6.0$ and $\varepsilon((SCN)_2^{\bullet-}) = 7600\ M^{-1}\ cm^{-1}$ (*G* represents yield of radicals per 100 eV of energy absorbed and ε the molar extinction coefficient at 475 nm). The dose delivered per pulse was within the range 5–80 Gy. The concentration of solute was kept in the range of $(0.5–10) \times 10^{-3}$ M. Details of the pulse radiolysis system were described previously [21].

2.7. Radiolysis of cryogenic glasses

The glassy samples of the 2-methyltetrahydrofuran (MTHF) and alcohol solutions were prepared by immersing the room-temperature solutions in liquid nitrogen. The samples were 0.5–3 mm thick and were placed in a temperature controlled, liquid nitrogen-cooled cryostat (Oxford Instruments). The desired temperature (77–150 K) was achieved by automatically controlled heating. The optical absorption spectra were measured on Cary 5 (Varian) spectrophotometer. The samples mounted in a cryostat were irradiated with 4 μs electron pulses from ELU-6 linear accelerator. Details of the matrix isolation technique are given elsewhere [22].

3. Results and discussion

3.1. The electrochemical reduction

Although the electrochemical reduction of azobenzene and related compounds is the subject of many papers [23] there is only a little information about the electrochemistry of heterocyclic azo dyes.

The aim of the electrochemical experiments is to study the reduction of the group of dyes **1**–**3** in EtOH and DMF solutions in order to compare the obtained data with the results of photochemical reduction. The detailed results of electrochemical experiments are presented in Table 3. In addition, the cyclic voltammograms of dyes **1** and **3** in both media are presented in Figs. 1 and 2.

In EtOH (Fig. 1A) two reduction peaks of the dye **1** exist. The first one present at −1.19 V corresponds to the ir-

Table 3
Cyclic voltammetric data[a] for the reduction of dyes **1**–**3** in DMF and EtOH

Dye	$E_{1/2}$[b]	$E_{pc(1)}$[c]	$E_{pc(2)}$	$E_{pc(3)}$	$E_{pc(4)}$	$E_{pa(1)}$	$E_{pa(2)}$	$E_{pa(3)}$	$E_{pa(4)}$
EtOH									
1	−1.16	−1.19	−2.20	–	–	–	−2.12	–	–
2	−1.20	−1.24	−2.20	–	–	–	−2.12	–	–
3	−0.90	−0.91	−1.30	−1.68	−2.21	−0.88	–	–	−2.12
DMF									
1	−1.37	−1.40	−1.99	−2.43	−2.65	−1.34	–	−2.37	−2.58
2	−1.45	−1.49	−2.21	–	–	−1.39	–	–	–
3	−1.06	−1.11	−1.53	−1.96	−2.44	−1.05	–	−1.88	−2.36

[a] All data [V]; $v = 0.1$ V/s.

[b] $E_{1/2}$ of the first electron transfer.

[c] (*n*) the number of the peak.

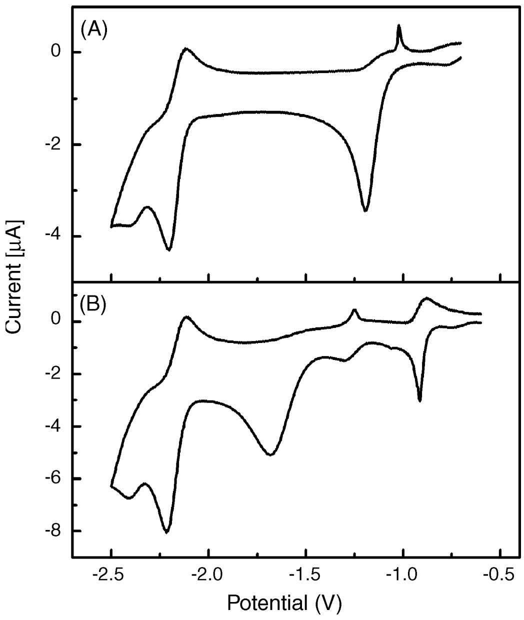

Fig. 1. Cyclic voltammograms of dye **1** (A) and **3** (B) in EtOH; scan rate (v) = 0.1 V/s.

reversible one-step two-electron process responsible for the reduction of the azo group. The second reduction peak at −2.20 V is assigned to the quasi-reversible reduction of the heterocyclic residue, by comparison to the voltammogram of the 2-aminobenzothiazole. The dye **2** exhibits very similar electrochemical behaviour in EtOH. On the other hand the reduction of the dye **3** in EtOH proceeds in five steps (Fig. 1B). The first three peaks present at −0.91 V (reversible), at −1.30 V (irreversible) and at −1.68 V (irreversible) are assigned to the reduction of the azo and the nitro groups. The last two reduction peaks at −2.21 and −2.40 V (deformed due to the electrolyte reduction) are responsible for the reversible and irreversible processes, probably the reduction of the heterocyclic residue. It is apparent from the obtained data that the presence of the nitro group lowers the reduction potential of the dye in comparison with the unsubstituted analogue.

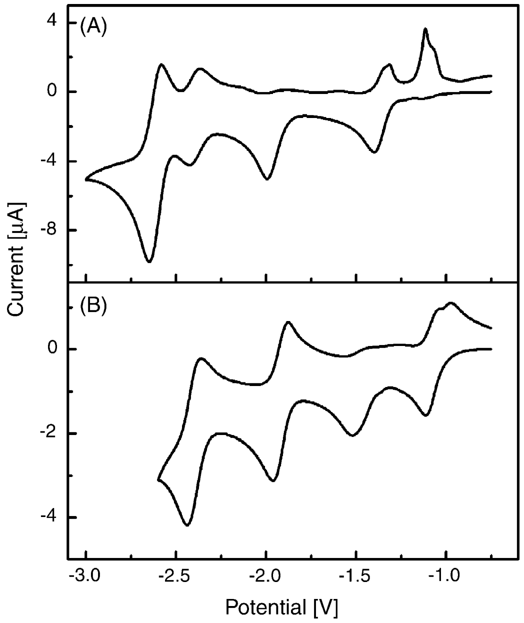

Fig. 2. Cyclic voltammograms of dye **1** (A) and **3** (B) in DMF; v = 0.1 V/s.

The voltammogram of the dye **1** in DMF (Fig. 2A) shows that its reduction proceeds in four steps. The first peak at −1.40 V (accompanied by an oxidation peak at −1.34 V) characterizes the reversible process, whereas the second peak at −1.99 V is responsible for the irreversible process; both of them are assigned to the reduction of the azo group. Two other peaks located at −2.43 and −2.65 V, accompanied by two oxidation peaks at −2.37 and −2.58 V, respectively, are assigned to the quasi-reversible steps of the heterocyclic moiety reduction. The voltammogram of the dye **2** in DMF shows two reduction peaks located at −1.49 and −2.21 V. The first one is accompanied by an oxidation peak located at −1.39 V. The obtained data indicate the quasi-reversible and irreversible character of both processes, respectively. The peaks of the reduction of heterocyclic residue are overlapped by peaks of the reduction of the electrolyte.

In the voltammogram of dye **3** in DMF (Fig. 2B) four peaks attributed to the reversible reduction ($v > 5$ V/s) appeared located at −1.11, −1.53, −1.96 and −2.44 V. The presence of the nitro group lowers the reduction potential of the analysed compound in the comparison with its unsubstituted analogue.

In both solvents, the dye **3** is more readily reduced than other dyes while the dye **2** is less readily reduced. This substitution effect can be related to the decreased/increased electron density at the azo group compared to the unsubstituted dye **1** what facilitates/makes more difficult its reduction.

The differences in electrochemical reduction of the investigated azo dyes in protic and aprotic solvents indicate different mechanism of the processes following reduction of the compound. In alcohol solution the attachment of an electron is accompanied by the protonation of the molecule (in radical anion form) while in DMF only a reduction in two one-electron steps enables protonation of the compound (in dianion form). These different mechanisms of the electrochemical reduction should also be reflected in photochemical reduction of the dyes in these solvents.

Our results indicate also that the dyes **1**–**3** are more readily reduced in EtOH than in DMF. In order to achieve the explanation of this fact the free energy of solvation of the dyes in both solvents was measured. MeOH was used instead of EtOH because the latter mixed to some extent with *n*-hexane used as immiscible solvent. Free energies of the transfer from alcohol or DMF to *n*-hexane (δG_{tr}) were determined by measuring the distribution coefficient γ (Table 4) of each dye in both phases at various temperatures [24]. The other thermodynamic data reported in Table 5 were calculated from Eq. (1):

$$\delta G_{\mathrm{tr}} = \delta H_{\mathrm{tr}} - T\delta S_{\mathrm{tr}} = -RT \ln \gamma \qquad (1)$$

Table 4
Distribution coefficients ($\gamma = C_{\text{sol}}/C_{n\text{-hexane}}$) of dyes **1**–**3** in solvents at different temperatures

	1	**2**	**3**
MeOH			
20 °C	4.68	2.71	5.46
25 °C	2.99	2.65	3.14
30 °C	2.20	2.50	1.98
35 °C	1.78	2.45	1.65
DMF			
20 °C	5.22	3.88	7.81
25 °C	4.26	2.99	5.90
30 °C	2.67	2.28	5.13
35 °C	2.49	2.27	4.42

The more negative values of δG_{tr} for dyes **1**–**3** in DMF indicate their stronger solvation in this medium [25,26]. Therefore an additional energy to reorganize the solvation shell around the dye molecule is needed in the reduction process. Moreover, there is the stronger dependence of the solvation on the chemical structures of the dyes **1**–**3** in DMF ($\delta G_{\text{tr}} = -2.71$ to -4.39 kJ/mol) in comparison with alcohol ($\delta G_{\text{tr}} = -2.41$ to -2.84 kJ/mol).

3.2. Pulse radiolysis experiments

The lowering of the reduction potential of the nitro-substituted dye **3**, which is confirmed by the results of electrochemical experiments and DFT calculations of electron affinities of substituted and unsubstituted species (see Table 2), should be also reflected by the efficiency of the electron attachment in reactions of the dyes with solvated electrons or other reducing species, as for example, ketyl radicals or acetone radical anions. However, by means of pulse radiolysis we have found that the rate constant for the reaction with solvated electrons is already diffusion controlled for **1** ($k \sim 1 \times 10^{10}$ M^{-1} s^{-1}), and therefore this reaction cannot confirm the higher reactivity of the nitro-substituted dyes derived from 2-aminobenzothiazole. Also, only the approximate values of the rate constants for the reactions with other reducing species can be found due to superpositions of electron transfer processes with the fast follow-up reactions of the radical anions formed. However, the decrease of the reduction potential of the molecule due to the substitution with an electron withdrawing nitro group is reflected by the observation of the reduction of **3** by $CH_2OH^{\bullet}$ radicals, generated radiolytically in liquid MeOH, whereas such reduction is not observed for **1**. We have found that this reaction, although much less effective than the reaction with 2-propanol ketyl radicals, unambiguously leads to the formation of the radical anion of **3** ($\mathbf{3}^{\bullet-}$). In neutral solution, initially formed $\mathbf{3}^{\bullet-}$ undergoes protonation to the neutral radical on the same time scale. The $CH_2OH^{\bullet}$ radicals are weak reducing species and react with most of the azo dyes through adduct formation rather than the one-electron reduction of the azo bond. Only strong decrease in the reduction potential due to substitution with the electron-withdrawing group, like in 4-nitroazobenzene or other nitro compounds, allows the one-electron reduction to be observed [27]. The presence of NO_2 group has also a pronounced effect on the reactivity of the radical anions formed in the reduction process. The changes in reactivity may not be limited only to the reactivity of the additional functional group. As pointed out by Neta and Meisel [28] the ability of the delocalization of an additional electron over the whole molecule, including the azo bond in the dyes, determines the efficiency of the electron transfer processes to nitroaromatics and therefore the reactivity of the whole radical anion formed.

Table 5
Thermodynamic quantities of transfer for dyes **1**–**3** from solvents to standard *n*-hexane at 25 °C

	δH_{tr} [kJ/mol]	δS_{tr} [J/mol K]	δG_{tr} [kJ/mol]
DMF			
1	−41.57	−128.87	−3.59
2	−27.71	−85.91	−2.71
3	−27.71	−77.60	−4.39
MeOH			
1	−41.57	−133.02	−2.71
2	−5.54	−11.08	−2.41
3	−83.14	−266.05	−2.84

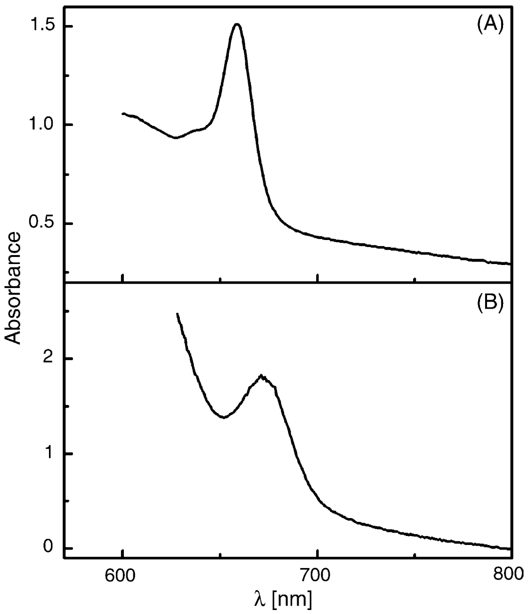

Fig. 3. Transient absorption spectra observed upon radiolysis of (A) **1** (0.01 M) and (B) **3** (0.01 M) in MTHF at 77 K; radiation dose 2.5 kGy; thickness of the sample 2.5 mm.

The electronic absorption spectra of radical anions generated radiolytically from **1** and **3** in MTHF matrix at 77 K are presented in Fig. 3. The shape of the band of radical anion of **1** is very similar to the absorption of the radical anion of 4-*N*,*N*-diethylaminoazobenzene (a strong low energy band accompanied by a shoulder at shorter wavelengths) and therefore may suggest similar negative charge distribution over the azo bond [29]. Only the maximum of the absorption of $\mathbf{1}^{\bullet-}$ is red shifted by over 15 nm compared to the radical anion of

4-*N*,*N*-diethylaminoazobenzene as a result of the substitution of the phenyl ring with the heterocyclic benzothiazole ring. If the heterocyclic ring is substituted with a strong electron-withdrawing nitro group a further red shift of the absorption band of the radical anion of **3**, compared with the absorption band of **1**$^{\bullet-}$, is observed.

On replacement of the aprotic MTHF solvent with alcohols the spectra of radical anions change significantly. The maxima of the absorption bands of both radical anions shift by over 20 nm towards shorter wavelengths as a result of hydrogen bonding. The maxima of the absorption bands of radical anions of **1** and **3** in 2-propanol at 77 K lie at 640 and 672 nm, respectively. These observations originating from experiments under cryogenic matrix conditions are confirmed by the spectra of radical anions obtained under basic conditions ([2-PrO$^-$Na$^+$] = 0.2 M) in liquid 2-propanol solutions (Fig. 4). Similar blue shift observed for **1**$^{\bullet-}$ and **3**$^{\bullet-}$ may suggest similar hydrogen bonding in both radical anions and may indicate an azo –N=N– bond as a target for hydrogen bond formation. In 4-*N*,*N*-diethylaminoazobenzene, hydrogen bonding caused more substantial shift of the absorption band of radical anion (around 40 nm) what may indicate weaker delocalizaton of the negative charge over the azo bond in the dyes derived from 2-aminobenzothiazole.

Upon softening of the alcoholic matrix on its annealing or generation of the radical anions of the dyes directly in alcoholic solution at lower pH, the radical anions undergo protonation [29]. In case of radical anions of **1** and **3** the products with similar absorption are observed. It indicates a formation of neutral radicals of similar structure. The spectra of the radicals formed in 2-propanol are presented in Fig. 5.

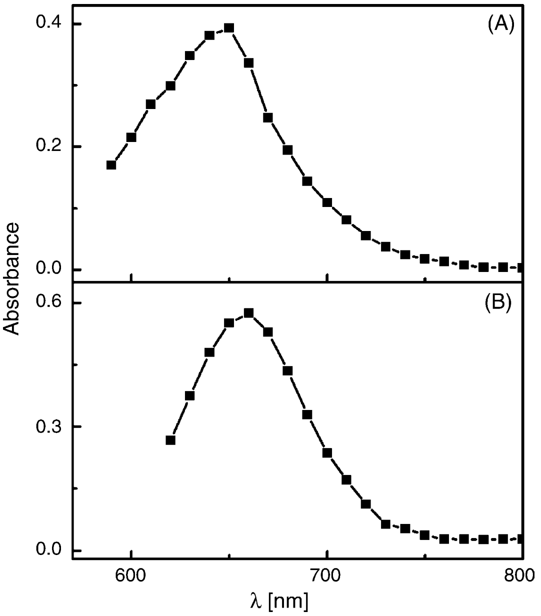

Fig. 4. Transient absorption spectra obtained by pulse radiolysis of N$_2$O-saturated basic solution ([*iso*-PrO$^-$Na$^+$] = 0.2 M) of dye (<0.01 M) in 2-propanol: (A) **1**, spectrum recorded 2 μs after the pulse; (B) **3**, spectrum recorded 4 μs after the pulse. The samples were 1 cm thick and received a radiation dose of 50 Gy.

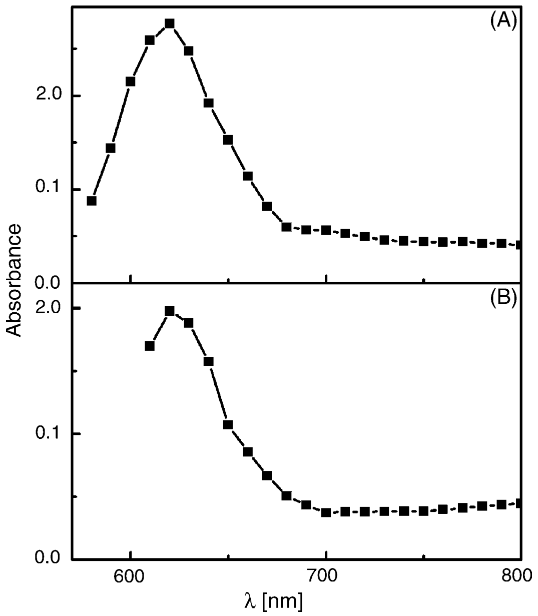

Fig. 5. Transient absorption spectra obtained by pulse radiolysis of N$_2$O-saturated neutral solution of dye (<0.01 M) in 2-propanol: (A) **1**; (B) **3**. Spectra recorded 8 μs after the pulse. The samples were 1 cm thick and received a radiation dose of 50 Gy.

The protonation of the radical anions of the investigated group of dyes can occur not only at the –N=N– azo bond, but also at the benzothiazole heterocycling ring (at the heteroatom sites), especially in the presence of strong electron withdrawing groups attached to the heterocycling moiety. Moreover, in **3**$^{\bullet-}$ the nitro group can undergo protonation itself. In fact, although the protonation of the radical anion generated from 2-aminobenzothiazole in MTHF under cryogenic conditions cannot be directly confirmed, the protonation process is observed for the radical anion of nitro-substituted 2-amino-6-nitrobenzothiazole upon matrix softening (data not shown). Therefore, the identification of the nature of the neutral radical formed on radical anion protonation is more difficult for the dyes derived from 2-aminobenzothiazole than from azobenzenes [27,29].

The DFT calculations at the B3LYP/6-31G* level were done to compare the relative stabilities of the possible structures of the neutral radicals. The calculation results presented in Table 6 indicate that the hydrazyl radical of the structure **1H**$^{\bullet}$ is the most stable. Therefore, we can assume that radical anions undergo protonation at the azo bond leading to hydrazyl radical, all the more that in alcohols this bond seems to be the primary target since it may be already hydrogen bonded to alcohol neighbor molecules.

The presence of the nitro group does not change this stability order of radicals. The protonation of the dye at the nitro group itself would lead to less stable product than the hydrazyl radicals. Additionally, very similar acidic properties of the radicals formed on protonation of **1**$^{\bullet-}$ and **3**$^{\bullet-}$,

Table 6
Relative energies of the dye radicals (in kcal/mol, relative to the most stable form)

Radical structures derived from **1**	ΔE	Radical structures derived from **3**	ΔE
$\text{Benzth-}\underset{\text{H}}{\underset{\mid}{\text{N}^\bullet}}\text{-N-PhN(Et)}_2$ **(1H•)**	(0)	$\text{O}_2\text{N-Benzth-}\underset{\text{H}}{\underset{\mid}{\text{N}^\bullet}}\text{-N-PhN(Et)}_2$ **(3H•)**	(0)
$\text{Benzth-}\underset{\text{H}}{\underset{\mid}{\text{N}}}\text{-N}^\bullet\text{-PhN(Et)}_2$	11.5	$\text{O}_2\text{N-Benzth-}\underset{\text{H}}{\underset{\mid}{\text{N}}}\text{-N}^\bullet\text{-PhN(Et)}_2$	11.6
$^\bullet\underset{\text{H(at nitrogen)}}{\underset{\mid}{\text{Benzth}}}\text{-N=N-PhN(Et)}_2$	7.2	$\text{O}_2\text{N-}^\bullet\underset{\text{H(at nitrogen)}}{\underset{\mid}{\text{Benzth}}}\text{-N=N-PhN(Et)}_2$	8.2
$^\bullet\underset{\text{H(at sulfur)}}{\underset{\mid}{\text{Benzth}}}\text{-N=N-PhN(Et)}_2$	35.6[a]	$\text{O}_2\text{N-}^\bullet\underset{\text{H(at sulfur)}}{\underset{\mid}{\text{Benzth}}}\text{-N=N-PhN(Et)}_2$	39.7[a]
		$\text{HO}_2\text{N}^\bullet\text{-Benzth-N=N-PhN(Et)}_2$	19.9

[a] Protonation of the radical anion of the dye at the sulphur atom leads to the scission of the S—C(aryl) bond.

as observed by pulse radiolysis experiments conducted under different pH conditions, can be understood in terms of a very modest effect of the stabilization of the anionic form by the contribution of the resonance structure $-\text{NO}_2^{\,-}$. This further confirms the assignment of the spectra presented in Fig. 5 to the species of similar radical structure. It is concluded that for the dyes derived from 2-aminobezothiazole, similar to the azobenzene dyes, the azo bond plays a key role upon reduction of the molecule.

3.3. Photochemical experiments

The results of the photochemical studies comprising the determination of the quantum yields of degradation of the examined dyes upon UV irradiation (300 nm) in EtOH and DMF solutions under anaerobic conditions and estimation of the light fastness on polyamide fibre are summarised in Table 7.

It is clear that the photodegradation of tested dyes **1–3** is strongly enhanced in DMF and retarded in alcohol. TLC analysis revealed that the irradiation of investigated colorants in these solvents generated both types of amines indicating the photoreduction process.

Providing the first step of photodegradation in alcohol is an electron transfer from the solvent to the excited molecule of the dye, followed by a fast protonation of the resulting dye radical anion, similar mechanism could be expected on polyamide, which is an electron donating environment [30]. The light fastness on the fibre remains consistent with the order of photostability of the dyes **1–3** in ethanol (see Table 7). We have previously shown that the influence of DMF can be more complex [31,32].

Table 7
The quantum yields Φ of photodegradation of the dyes **1–3**

Dye	EtOH, Φ ($\times 10^4$)	DMF, Φ ($\times 10^4$)	Light fastness
1	0.94	8.0	5–6
2	0.42	14.0	6
3	9.04	136.0	2

It is apparent from the presented results that the tendency to the electrochemical reduction in EtOH remains similar on photoexcitation, resulting in close relation between electrochemical reduction potentials and photochemical quantum yields of degradation of the dyes (compare Tables 3 and 7).

4. Conclusions

The parallel tendency to the electrochemical and photochemical reduction of some azo dyes in alcohol was found. This can be explained on the basis of quantum chemical calculations of the electron affinities in the ground and excited states. Although the $-\text{NO}_2$ group can play the important role in the one-electron reduction process it is the central azo bond which accommodates mainly an additional electron and is further protonated into the hydrazyl radical.

Acknowledgements

We thank Dr. Paweł Bednarek (University of Fribourg, Switzerland) for helpful discussion. This work was supported by the Polish Committee of Scientific Research, project no. 4 T09B 11522.

References

[1] J.F. Ready, Kirk–Othmer Encyclopedia of Chemical Technology, vol. 14, 3rd ed., Wiley, New York, 1986, pp. 42–81.
[2] S.R. Leone, C.B. Moore, in: C.B. Moore (Ed.), Chemical and Biochemical Application of Lasers, vol. 1, Academic Press, New York, 1974, pp. 12–15.
[3] K.-Y. Law, Chem. Rev. 93 (1993) 449–486.
[4] P. Gregay, Rev. Prog. Color. 14 (1994) 1–7.
[5] G.S. Egerton, A.G. Morgan, J. Soc. Dyers Colour 86 (1970) 242–246.

[6] C.H. Giles, D.G. Duff, R.S. Sinclair, Rev. Prog. Color. 12 (1982) 58–65.

[7] C.H. Giles, S.D. Forrester, in: N.S. Allen, J.F. McKellar (Eds.), Photochemistry of Dyed and Pigmented Polymers, Elsevier, London, 1980, p. 51.

[8] B. Milligan, Rev. Prog. Color. 16 (1986) 1–7.

[9] K. McLaren, Can. Tex. J. 76 (1959) 41–46.

[10] K. McLaren, J. Soc. Dyers Colour 78 (1962) 34–38.

[11] N.A. Evans, in: N.S. Allen, J.F. McKellar (Eds.), Photochemistry of Dyed and Pigmented Polymers, Elsevier, London, 1980, pp. 93–103.

[12] P.J. Hillson, E. Rideal, Proc. Roy. Soc. (Lond.) A216 (1953) 458–466.

[13] M.F. Sartori, J. Soc. Dyers Colour 83 (1967) 144–153;
M.F. Sartori, United States Patent. 3,405,118 (1968);
H.A. Weaver, D.J. Wallace, United States Patent. 3,423,394 (1969).

[14] A.D. Becke, J. Chem. Phys. 98 (1993) 5648–5652.

[15] C. Lee, W. Yang, R.G. Parr, Phys. Rev. B 37 (1988) 785–789.

[16] M.J. Frisch, G.W. Trucks, H.B. Schlegel, G.E. Scuseria, M.A. Robb, J.R. Cheeseman, V.G. Zakrzewski, J.A. Montgomery, R.E. Stratmann, J.C. Burant, S. Dapprich, J.M. Millam, A.D. Daniels, K.N. Kudin, M.C. Strain, O. Farkas, J. Tomasi, V. Barone, M. Cossi, R. Cammi, B. Mennucci, C. Pommelli, C. Adamo, S. Clifford, J. Ochterski, G.A. Petersson, P.Y. Ayala, Q. Cui, K. Morokuma, D.K. Malicki, A.D. Rabuck, K. Raghavachari, J.B. Foresman, J. Cioslowski, J.V. Ortiz, B.B. Stefanov, G. Liu, A. Liashenko, P. Piskorz, I. Komaromi, R. Gomperts, R.L. Martin, D.J. Fox, T. Keith, M.A. Al.-Laham, C.Y. Peng, A. Nanayakkara, M. Challacombe, P.M.W. Gill, B.G. Johnson, W. Chen, M.W. Wong, J.L. Andres, C. Gonzales, M. Head-Gordon, E.S. Repogle, J.A. Pople, Gaussian 98, Rev. A.1, Gaussian, Inc., Pittsburgh, PA, 1998.

[17] M. Seralathan, R.A. Osteryoung, J.G. Osteryoung, J. Electroanal. Chem. 222 (1987) 69–78.

[18] J.F. Coetzee, J.J. Campion, J. Am. Chem. Soc. 89 (1967) 2513–2517.

[19] H. Schneider, H. Strehlow, J. Electroanal. Chem. 12 (1966) 530–534.

[20] W.B. Leighton, G.S. Forbes, J. Am. Chem. Soc. 52 (1930) 3139–3152.

[21] S. Karolczak, K. Hodyr, R. Łubis, J. Kroh, J. Radioanal. Nucl. Chem. 101 (1986) 177–188;
S. Karolczak, K. Hodyr, M. Połowinski, Radiat. Phys. Chem. 3 (1992) 1–5.

[22] T. Bally, in: A. Lund, M. Shiotani (Eds.), Radical Ionic Systems, Kluwer Academic Publishers, Dordrecht, 1991, pp. 3–54;
J. Gębicki, A. Marcinek, in: Z.B. Alfassi (Ed.), General Aspects of the Chemistry of Radicals, Wiley, Chichester, 1999, pp. 175–208.

[23] X. Peng, J. Yang, J. Wang, Dyes Pigm. 20 (1992) 73–81;
P. Savarino, G. Viscardi, E. Barini, E. Montoneri, P. Quagliotto, Dyes Pigm. 20 (1992) 1–11.

[24] E. Buncel, H. Wilson, Acc. Chem. Res. 12 (1979) 42–48;
E. Buncel, H. Wilson, J. Chem. Ed. 57 (1980) 629–633.

[25] A. Arcoria, H.L. Longo, E. Maccarone, G. Parisi, G. Perrini, J. Soc. Dyers Colour 100 (1984) 13–16.

[26] I.J. Wang, P.Y. Wang, Textile Res. J. 60 (1990) 297–300.

[27] S. Monti, L. Flamigni, J. Phys. Chem. 90 (1986) 1179–1184.

[28] P. Neta, Meisel, J. Phys. Chem. 80 (1976) 519–524.

[29] R. Podsiadły, J. Sokołowska, A. Marcinek, J. Zielonka, M. Czerwińska, A. Sikora, J. Photochem Photobiol. A: Chem. 163 (2004) 373–379.

[30] N.S. Allen, J.F. McKellar, D. Wilson, Makromol. Chem. 179 (1979) 269–271.

[31] J. Sokołowska, W. Czajkowski, R. Podsiadły, Dyes Pigm. 49 (2001) 187–191.

[32] R. Podsiadły, J. Sokołowska, A. Marcinek, J. Zielonka, E. Chrześcijańska, A. Socha, Color. Tech. 119 (2003) 269–274.